Science Advances
AAAS

Supplementary Materials for

Coactivator condensation drives cardiovascular cell lineage specification

Peiheng Gan *et al.*

Corresponding author: Eric N. Olson, eric.olson@utsouthwestern.edu;
Benjamin R. Sabari, benjamin.sabari@utsouthwestern.edu

Sci. Adv. **10**, eadk7160 (2024)
DOI: 10.1126/sciadv.adk7160

This PDF file includes:

Figs. S1 to S10

Fig. S1

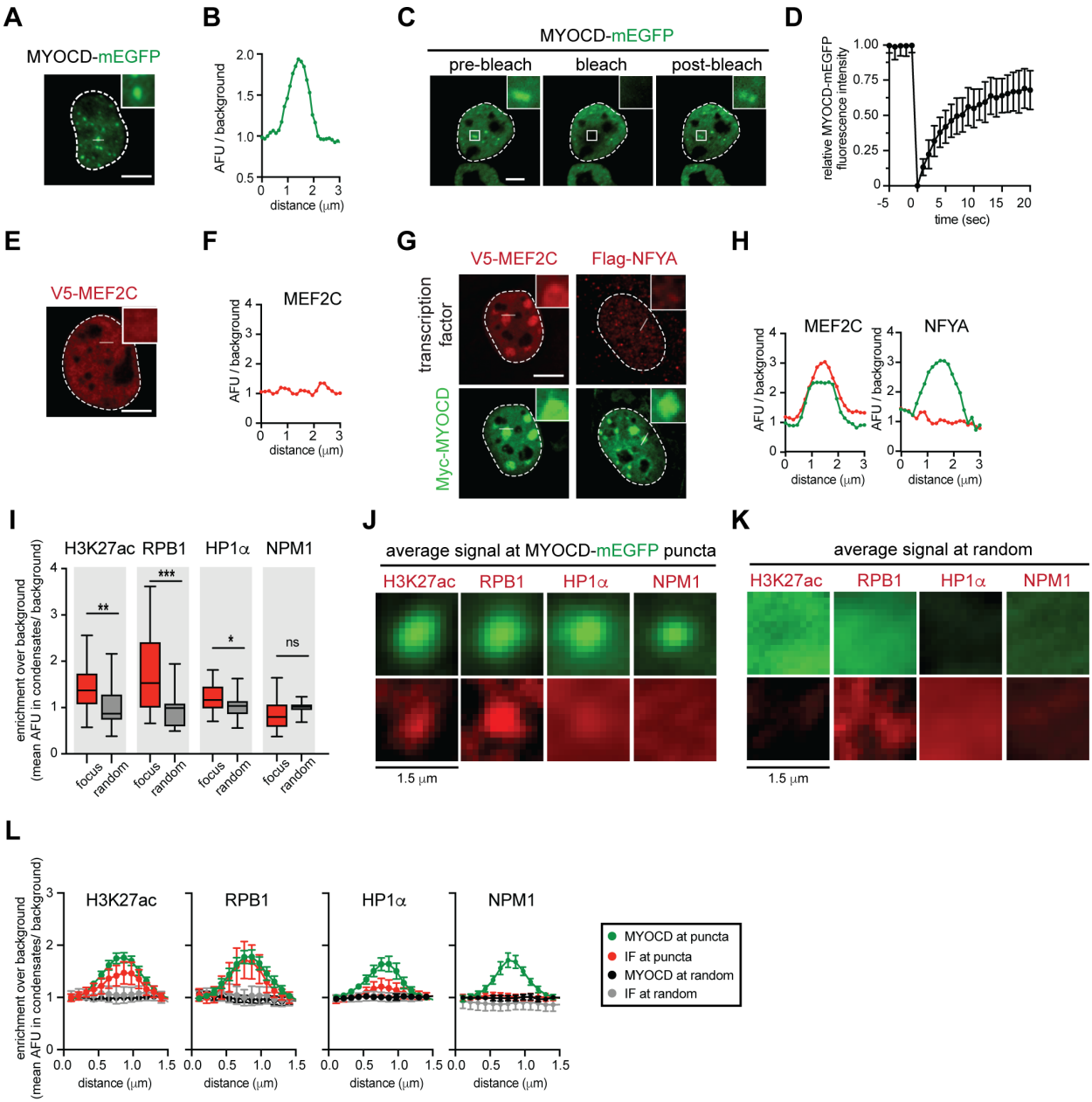

Fig. S1 MYOCD nuclear condensates colocalize with active transcriptional components.
(A) Representative micrograph (max projections) of COS-7 cells expressing MYOCD-mEGFP. Dotted line defines nucleus. White line denotes line profile in **fig. S1B** and is the location of crop shown in top right. Scale, 5 μm. **(B)** Line profile plot presented as AFU/background across the 3μm white line shown in **fig. S1A. (C)** Micrographs representing COS-7 cells expressing MYOCD-mEGFP during fluorescence recovery after photobleaching (FRAP). Square box denotes location of crop shown in top right. Scale, 5 μm. n=10. **(D)** Quantification of data in **fig. S1C** for normalized MYOCD-mEGFP signal over time. Data shown as mean ± SD. **(E)** IF imaging of V5-tagged MEF2C expressed in COS-7 cells with V5 antibody targeting the epitopes. White line denotes line profile in **fig. S1F** and is the location of crop shown in top right. Scale bar, 5μm. **(F)**

Line profile plot presented as AFU/background across the 3µm white line shown in **fig. S1E**. **(G)** IF imaging of Myc-tagged MYOCD and other transcription factors (V5-tagged MEF2C and Flag-tagged NFYA) co-expressed in COS-7 cells. Scale bar, 5µm. **(H)** Line profile plot presented as AFU/background for either MYOCD (green) or the indicated co-expressed transcription factor (red) across the 3µm white line shown in **fig. S1G. (I)** Boxplot (mean ± min.-max.) showing enrichment of respective factors at either the center of the MYOCD-mEGFP focus or at random sites in COS-7 cells. p values represent results of t test (p values: ns $p>0.05$, * $p<=0.05$, ** $p <= 0.01$, *** $p<=0.001$). n=30. **(J)** Average signal of indicated factor (red) or MYOCD (GFP) centered at the MYOCD-mEGFP focus (1.5 μm^2) in COS-7 cells. **(K)** Average signal of indicated factor (red) or MYOCD (GFP) centered at random locations in COS-7 cells. **(L)** Graph showing line profile of relative factor enrichment centered at MYOCD-mEGFP focus (green) or at random (black) and indicated factor centered at focus (red) or at random (gray). Data shown as mean ± SEM.

Fig. S2

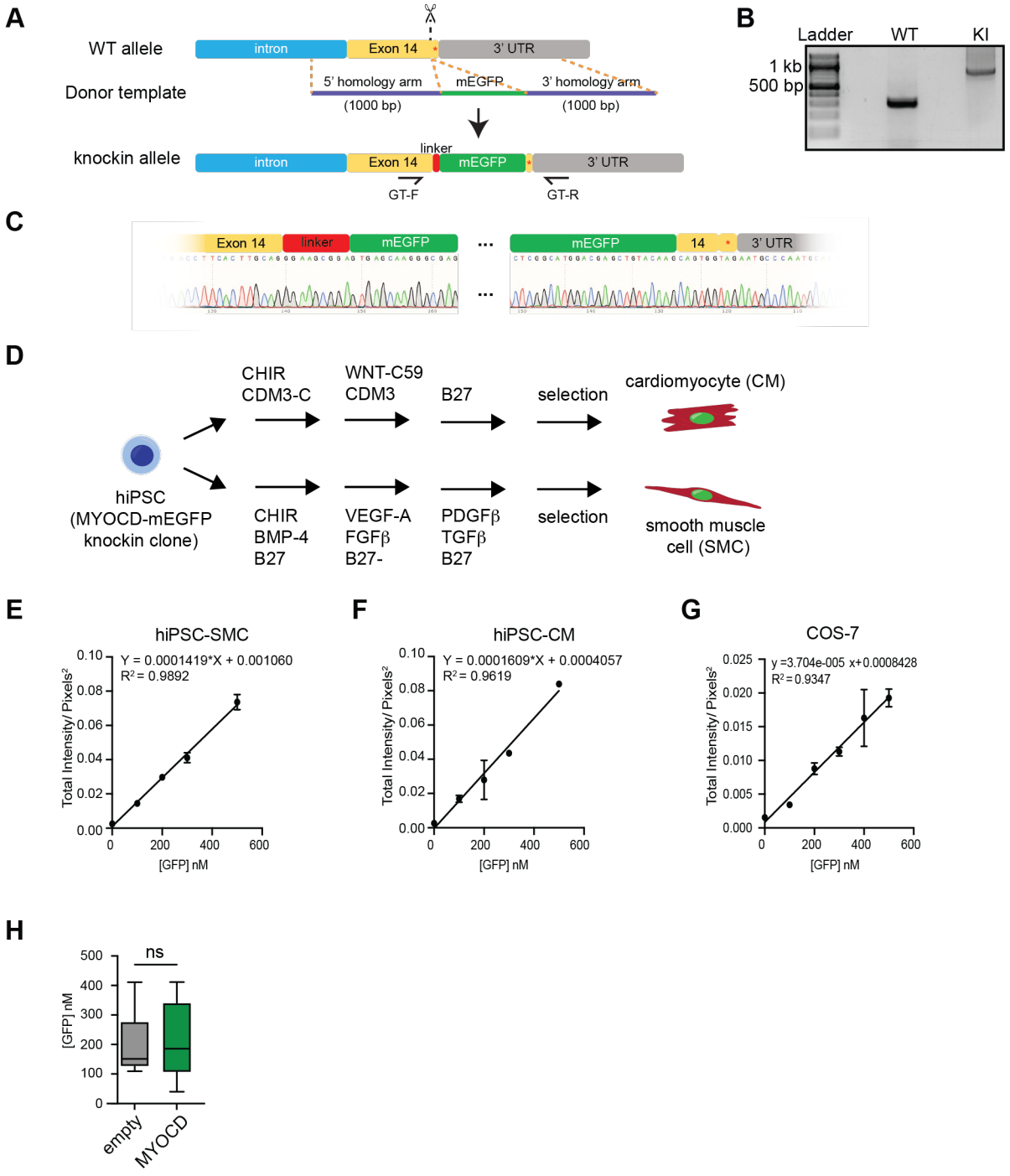

Fig. S2 Generation and utilization of MYOCD-mEGFP knock-in hiPSC line to model MYOCD function during cell lineage specification.

(A) Schematic of experimental design to knock in mEGFP sequence into MYOCD Exon 14 by CRISPR-Cas9-mediated homology directed repair (HDR). Donor template is shown. Black arrows

indicate PCR genotyping primers, GT-F and GT-R. **(B)** Gel electrophoresis of PCR product using genomic DNA from parental or knock-in clone with genotyping primers to confirm the homozygous MYOCD-mEGFP knock-in in an isogenic hiPSC clone. Band size: WT 319 bp, KI 1,042 bp. **(C)** Sequencing tracks showing the 5' and 3' regions of mEGFP knock-in sites in MYOCD Exon 14. **(D)** Schematic of SMC and CM differentiation protocols from hiPSCs. **(E)** Scatter plot (mean ± SD) of fluorescence intensity/pixels^2 by concentration of purified, recombinant mEGFP for hiPSC to SMC. Data shown as mean ± SD, r^2= goodness-of-fit for linear regression. n=3. **(F)** Scatter plot (mean ± SD) of fluorescence intensity/pixels^2 by concentration of purified, recombinant mEGFP for hiPSC to CM. Data shown as mean ± SD, r^2 = goodness-of-fit for linear regression. n=3. **(G)** Scatter plot (mean ± SD) of fluorescence intensity/pixels^2 by concentration of purified, recombinant mEGFP. Data shown as mean± SD, r^2 = goodness-of-fit for linear regression. n=3. **(H)** Box plot (min.-max) of the concentration of mEGFP (nM) in COS-7 cells analyzed in **Fig. 2, E and F.** p values represent results of t test (p values: ns $p>0.05$).

Fig. S3

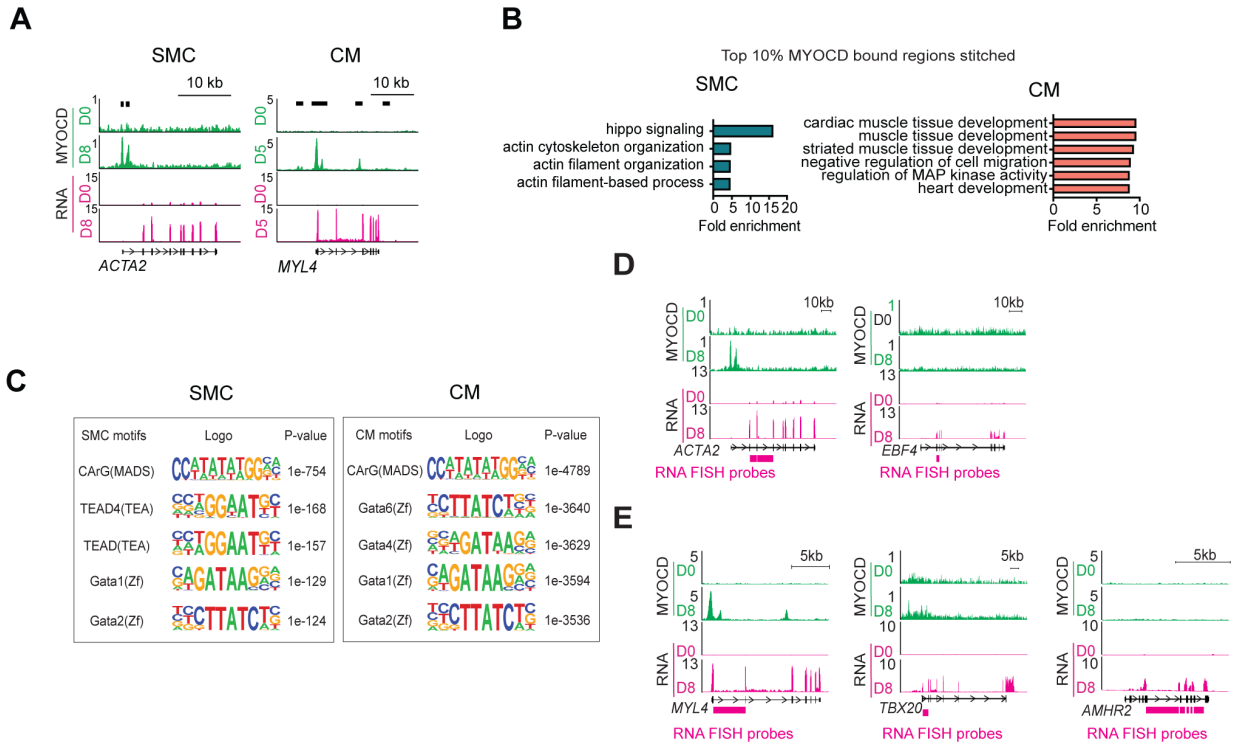

Fig. S3 MYOCD ChIP-seq during SMC and CM lineage specification.

(A) Gene tracks of MYOCD ChIP-seq and RNA-seq from undifferentiated iPSCs (D0), meso-SMCs (D8), and meso-CMs (D5). The black bars represent MYOCD peaks. **(B)** Gene ontology analysis of annotated genes within the top 10% of MYOCD bound regions using the stitching method (as described in methods) for both SMC (left) and CM (right). **(C)** Enriched motifs identified using Homer for MYOCD peak regions (summit ± 20bp) for both SMC (D8) (left) and CM (D5) (right) samples. **(D)** Gene tracks for MYOCD ChIP-seq and RNA-seq from undifferentiated iPSCs and meso-SMC (D8) cells for the RNA-FISH candidates. The location of FISH probe is shown as pink bars. **(E)** Gene tracks for MYOCD ChIP-seq and RNA-seq from undifferentiated and meso-CM (D5) cells for the RNA-FISH candidates. The location of FISH probe is shown as pink bars.

Fig. S4

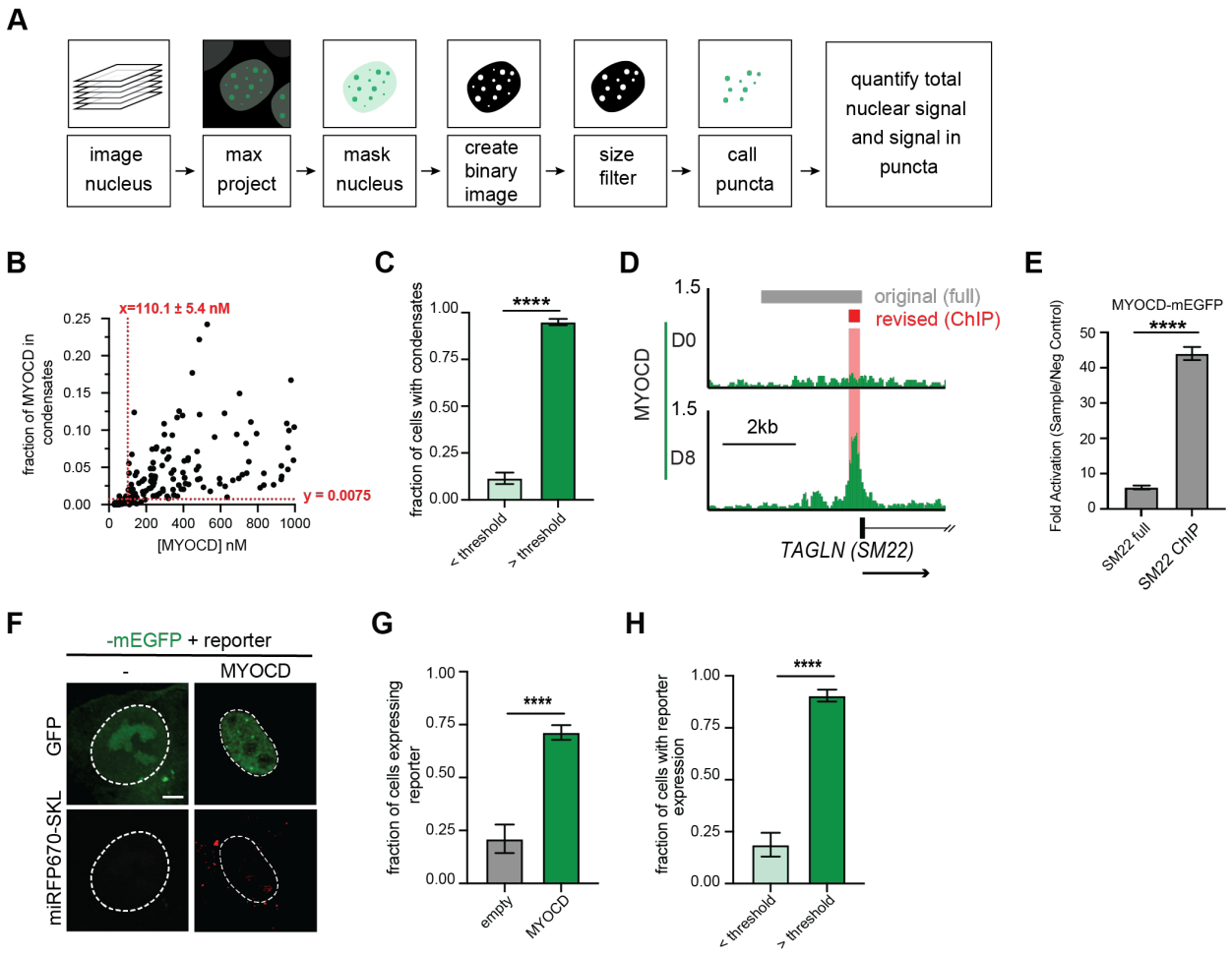

Fig. S4 Quantification of MYOCD condensate formation and gene activation.
(A) Illustration of the custom, semiautomated CellProfiler pipeline used to analyze micrographs. **(B)** Scatter plot of the raw data output where each dot represents one nucleus. Data are plotted as the fraction of MYOCD signal in condensates divided by the total fluorescence within the nucleus (Y axis) correlated with nuclear concentration of MYOCD (X axis). X denotes the concentration threshold from simple logarithmic regression previously mentioned. Y equals the cutoff for condensates (1) or no condensates (0) to account for image artifacts. **(C)** Bar chart (mean ± SEM) displaying the fraction of cells below the critical concentration threshold or above the critical concentration threshold that form condensates. p value is from t test (p values: **** p<=0.0001). Data represented relates to **Fig. 4, B and C**. 5 biological replicates. n=292. **(D)** Gene tracks for MYOCD ChIP-seq from undifferentiated iPSCs (D0) and meso-SMC (D8) cells for the *TAGLN* (*SM22*) gene. The location of *SM22* promoter is shown as long gray bar (original) and short red bar (ChIP peak). **(E)** Bar chart (mean ± SD) displaying relative fold luciferase reporter activation of full *SM22* promoter compared to *SM22* MYOCD-ChIP peak. Reporter expression is normalized to GFP only control. p value is from t test (p values: **** p<0.001) n=3. **(F)** Representative micrographs (max projections) of COS-7 cells expressing MYOCD-mEGFP or mEGFP and the fluorescent reporter (miRFP670-SKL, signal shown in red). Brightness and contrast of displayed

micrographs are equivalent. Scale, 5 μm. n~20. **(G)** Bar chart of the fraction of cells expressing the reporter above the concentration threshold determined in **Fig. 4F.** Data shown as bar chart (mean ± SEM) p values from Mann Whitney test, **** p<=0.0001. **(H)** Bar chart (mean ± SEM) displaying the fraction of cells below the critical concentration threshold or above the critical concentration threshold that express the reporter. p value is from t test (p values: **** p<=0.0001). Data represented relates to **Fig. 4, E and F**.

Fig. S5

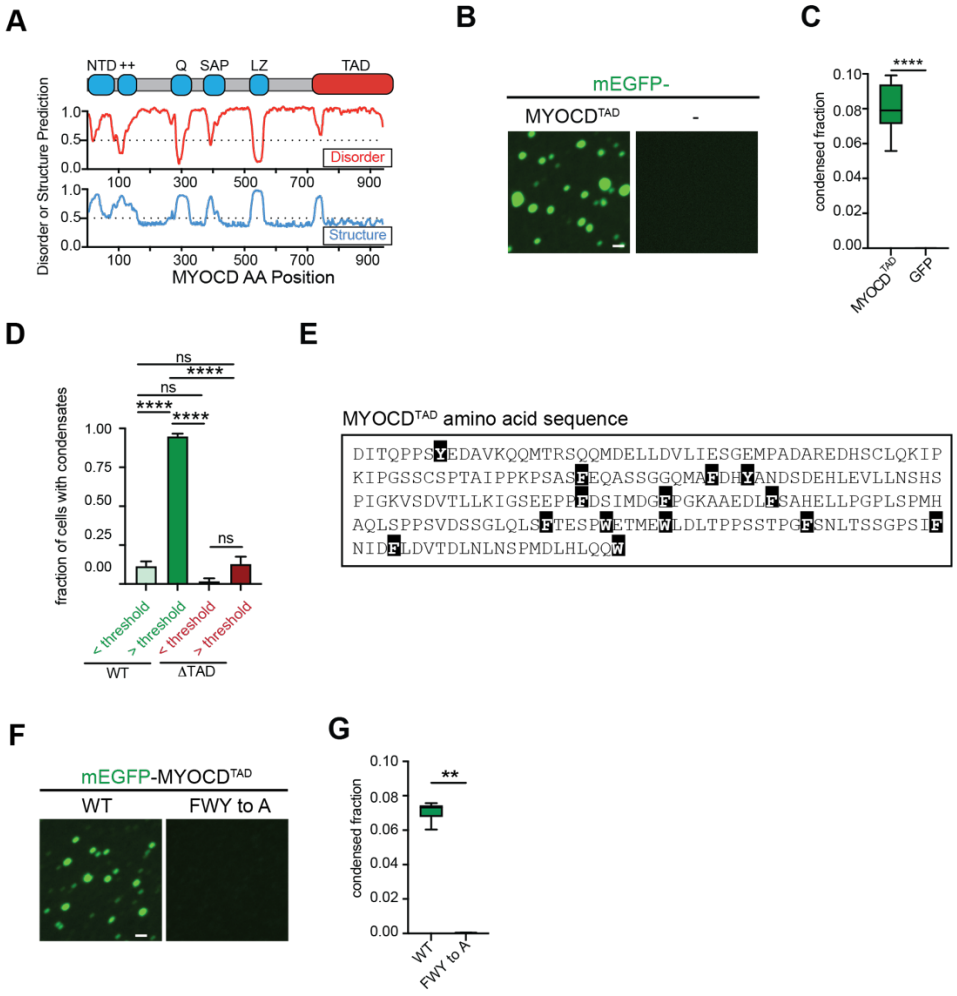

Fig. S5 TAD is required for MYOCD condensate formation.

(A) Disorder and structure prediction plots from Metapredict (bottom) annotated with MYOCD known domains (top), N terminal domain (NTD), two helices containing several highly conserved positively charged residues (++), a stretch of glutamine (Q), SAF-A/B, Acinus, PIAS domain (SAP), leucine zipper (LZ), and transcription activation domain (TAD). **(B)** Representative micrographs of *in vitro* condensate formation of MYOCD^{TAD} fused to mEGFP or mEGFP alone in protein storage buffer (50 mM Tris, 75 mM NaCl, 5% glycerol, 1mM PMSF, 1 mM DTT) and 20% PEG. Scale, 5µm. n=8. **(C)** Box plot (10%-90%) of condensed fraction. p values represent results of t test (p values: **** p<=0.0001). **(D)** Bar chart (mean ± SEM) displaying the fraction of cells below the critical concentration threshold or above the critical concentration threshold that form condensates. p value is from one-way ANOVA with Dunn's multiple comparison test (p values: **** p<=0.0001). Data represented relates to **Fig. 5, A to C**. **(E)** Graphical representation of the MYOCD^{TAD} amino acid sequence with aromatic residues in black boxes. **(F)** Representative micrographs of *in vitro* condensate formation of MYOCD^{TAD} fused to mEGFP or aromatic to alanine MYOCD^{TAD} in protein storage buffer (50 mM Tris, 75 mM NaCl, 5% glycerol, 1mM

PMSF, 1 mM DTT) and 20% PEG. Scale, 5μm. n=5. **(G)** Box plot (10%-90%) of condensed fraction. p values represent results of t test (p values: ** $p <= 0.01$).

Fig. S6

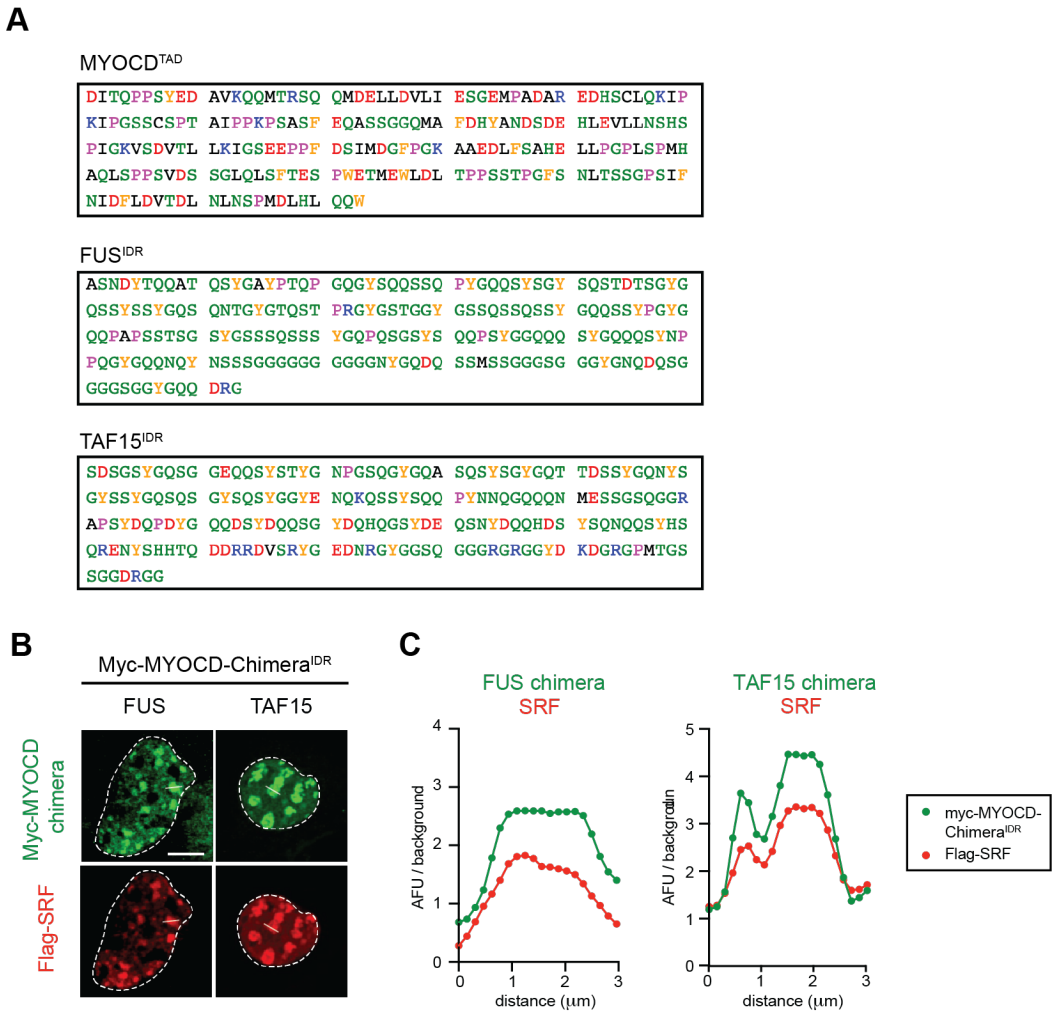

Fig. S6 MYOCD chimeric fusions recapitulate the capacity of concentrating transcription factors.

(A) Amino acid sequences of MYOCD^{TAD}, FUS^{IDR} and TAF15^{IDR}. **(B)** IF imaging of MYOCD-Chimera^{IDR}-mEGFP (FUS and TAF15) and Flag-tagged SRF co-expressed in COS-7 cells. Scale, 5µm. Dash line marks nucleus. **(C)** Line profile plot presented as AFU/background for the indicated MYOCD chimeric fusion (green) or co-expressed SRF (red) across the 3µm white line shown in **fig. S6B.**

Fig. S7

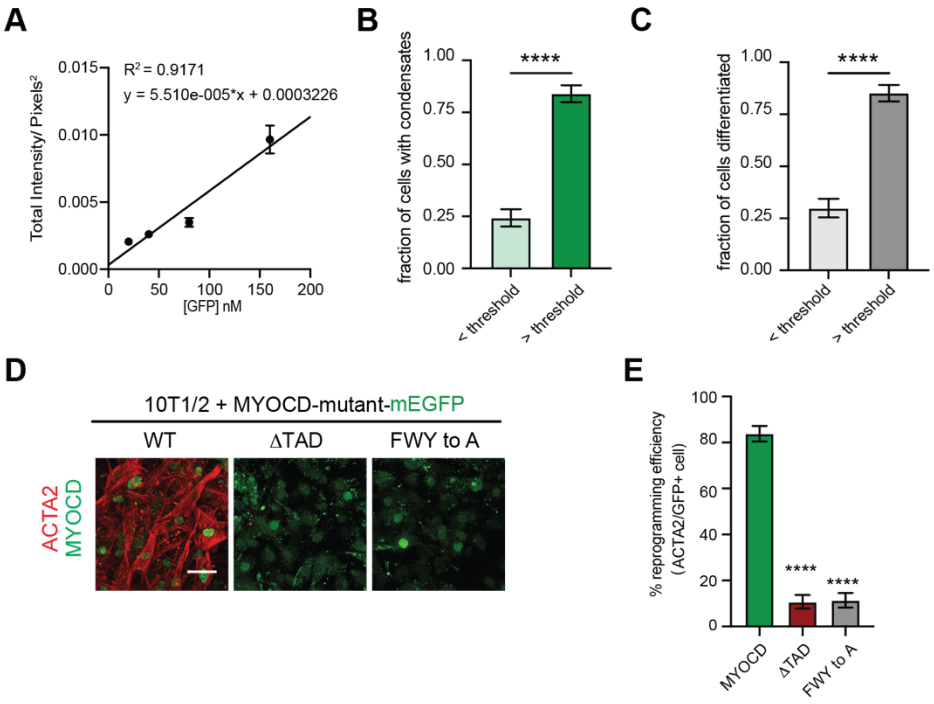

Fig. S7 MYOCD forms condensates in the reprogramming assay.
(A) Scatter plot (mean ± SD) of fluorescence intensity/ pixels^2 by concentration of purified, recombinant mEGFP. Data shown as mean ± SD, r^2= goodness-of-fit for linear regression. n=3. **(B)** Bar chart (mean ± SEM) displaying the fraction of cells below the critical concentration threshold or above the critical concentration threshold that form condensates. p value is from t test (p values: **** p<=0.0001). Data represented relates to **Fig. 6, B and C. (C)** Bar chart displaying the fraction of cells below the critical concentration threshold or above the critical concentration threshold that reprogram to SMCs. p value is from t test (p values: **** p<=0.0001). Data represented relates to **Fig. 6, B and C. (D)** Representative micrographs of 10T1/2 cells expressing MYOCD WT, ΔTAD, or FWY to A mutant (green). IF for ACTA2 (red) denotes SMC differentiation. Brightness and contrasting of displayed micrographs are equivalent. Scale, 50 µm. n=3. **(E)** Bar chart of the percentage of 10T1/2 cells reprogrammed to SMC. Data shown as mean ± SEM, p values from one-way ANOVA with Dunn's test, **** p<=0.0001.

Fig. S8

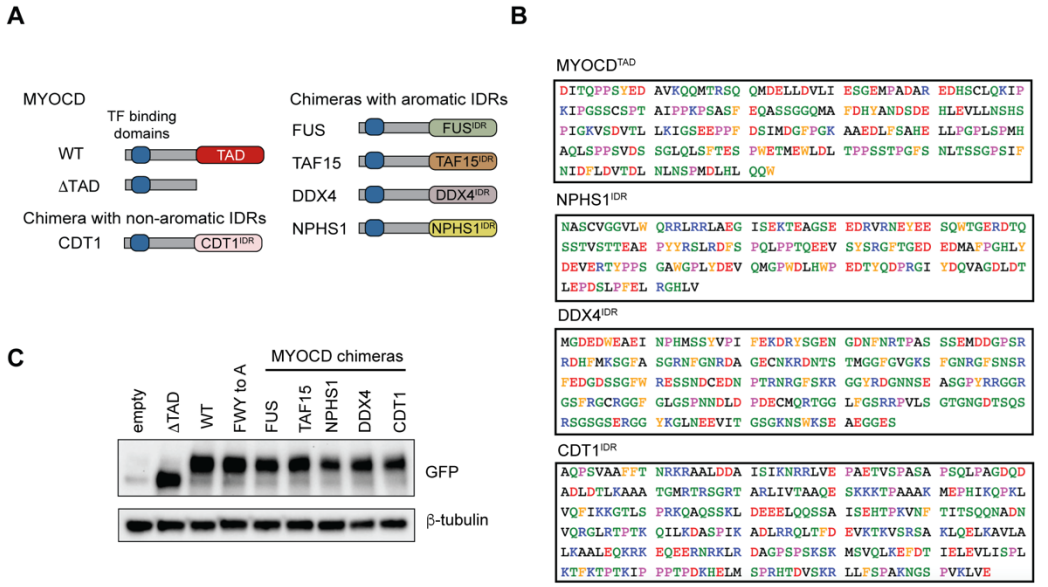
A
MYOCD
TF binding domains
WT
TAD
ΔTAD
Chimera with non-aromatic IDRs
CDT1
CDT1IDR
Chimeras with aromatic IDRs
FUS
FUSIDR
TAF15
TAF15IDR
DDX4
DDX4IDR
NPHS1
NPHS1IDR
B
MYOCDTAD
DITQPPSYED AVKQQMTRSQ QMDELLDVLI ESGEMPADAR EDHSCLQKIP
KIPGSSCSPT AIPPKPSASF EQASSGGQMA FDHYANDSDE HLEVLLNSHS
PIGKVSDVTL LKIGSEEPPF DSIMDGFPGK AAEDLFSAHE LLPGPLSPMH
AQLSPPSVDS SGLQLSFTES PWETMEWLDL TPPSSTPGFS NLTSSGPSIF
NIDFLDVTDL NLNSPMDLHL QQW
NPHS1IDR
NASCVGGVLW QRRLRRLAEG ISEKTEAGSE EDRVRNEYEE SQWTGERDTQ
SSTVSTTEAE PYYRSLRDFS PQLPPTQEEV SYSRGFTGED EDMAFPGHLY
DEVERTYPPS GAWGPLYDEV QMGPWDLHWP EDTYQDPRGI YDQVAGDLDT
LEPDSLPFEL RGHLV
DDX4IDR
MGDEDWEAEI NPHMSSYVPI FEKDRYSGEN GDNFNRTPAS SSEMDDGPSR
RDHFMKSGFA SGRNFGNRDA GECNKRDNTS TMGGFGVGKS FGNRGFSNSR
FEDGDSSGFW RESSNDCEDN PTRNRGFSKR GGYRDGNNSE ASGPYRRGGR
GSFRGCRGGF GLGSPNNDLD PDECMQRTGG LFGSRRPVLS GTGNGDTSQS
RSGSGSERGG YKGLNEEVIT GSGKNSWKSE AEGGES
CDT1IDR
AQPSVAAFFT NRKRAALDDA ISIKNRRLVE PAETVSPASA PSQLPAGDQD
ADLDTLKAAA TGMRTRSGRT ARLIVTAAQE SKKKTPAAAK MEPHIKQPKL
VQFIKKGTLS PRKQAQSSKL DEEELQQSSA ISEHTPKVNF TITSQQNADN
VQRGLRTPTK QILKDASPIK ADLRRQLTFD EVKTKVSRSA KLQELKAVLA
LKAALEQKRK EQEERNRKLR DAGPSPSKSK MSVQLKEFDT IELEVLISPL
KTFKTPTKIP PPTPDKHELM SPRHTDVSKR LLFSPAKNGS PVKLVE
C
MYOCD chimeras
empty
ΔTAD
WT
FWY to A
FUS
TAF15
NPHS1
DDX4
CDT1
GFP
β-tubulin
D
10T1/2 + MYOCD-mutant-mEGFP
WT
ΔTAD
FUS
TAF15
DDX4
NPHS1
CDT1
ACTA2
MYOCD
E
% reprogramming efficiency (ACTA2/GFP+ cell)
MYOCD Chimeras
F
10T1/2 + MYOCD-mutant-mEGFP
ACTA2
MYOCD
MYOCD
G
Condensates
fraction of cells above threshold with condensates
MYOCD Chimeras
H
Differentiation
fraction of cells above threshold differentiated
MYOCD Chimeras
I
Acta2
relative expression
empty
WT
ΔTAD
FWYtoA
MYOCD Chimeras
J
SMC genes
Fold Activation (Sample FPKM/ Average control FPKM)
empty
WT
ΔTAD
FUS
CDT1

Fig. S8 MYOCD chimeric fusions reprogram 10T1/2 into SMC.
(A) Schematic of WT MYOCD and MYOCD truncations and chimeras expressed in 10T1/2 cells. **(B)** Amino acid sequences of $MYOCD^{TAD}$, $DDX4^{IDR}$, $NPHS1^{IDR}$ and $CDT1^{IDR}$. Sequences for IDRs of FUS and TAF15 are presented in **fig. S6A**. **(C)** Western blot analysis of 10T1/2 cells expressing MYOCD WT (~180 kDa), ΔTAD (~150 kDa) or indicated chimeras (~180 kDa). β-tubulin (~55 kDa) was used as a loading control. **(D)** Representative micrographs of 10T1/2 cells overexpressing indicated construct (green). Immunofluorescence for ACTA2 (red) denotes SMC differentiation. Brightness and contrasting of displayed micrographs are equivalent. Scale, 50 μm. n, 3. **(E)** Bar chart of the percentage of 10T1/2 cells reprogrammed to SMC. Data shown as mean ± SEM, p values from one-way ANOVA with Dunn's test, * p <= 0.05, ** p <= 0.01, **** p<=0.0001. **(F)** Representative micrographs (max projections) of 10T1/2 cells expressing MYOCD-mEGFP (green) and indicated chimeric mutants. IF for ACTA2 (red) denotes SMC differentiation. Brightness and contrast of displayed micrographs are equivalent. Scale, 5 μm. Bottom row is zoomed in to highlight MYOCD condensates and only the GFP channel is presented. **(G** and **H)** Bar chart (mean ± SEM) displaying the fraction of cells above the critical MYOCD concentration threshold that form condensates (**g**) or differentiated (**h**). p value is from one-way ANOVA with Dunn's multiple comparison test (p values: ns p>=0.05, **** p<=0.0001). n~40. **(I)** Bar chart (mean ± SD) of relative expression of *Acta2* from qRT-PCR using 10T1/2 cells expressing MYOCD-mEGFP or indicated mutant. p values from one-way ANOVA with Dunnett's test. (p values: ns p>0.05, ** p <= 0.01, *** p <= 0.001, **** p<=0.0001). **(J)** Box plot (10%-90%) displaying the fold change of expression of SMC genes used in heatmap in **Fig. 6L** normalized to the empty vector control. p value is from Kruskal-Wallis test with Dunn's multiple comparison test (p values: ns p>0.05, n**** p<=0.0001). n=24 genes.

Fig. S9

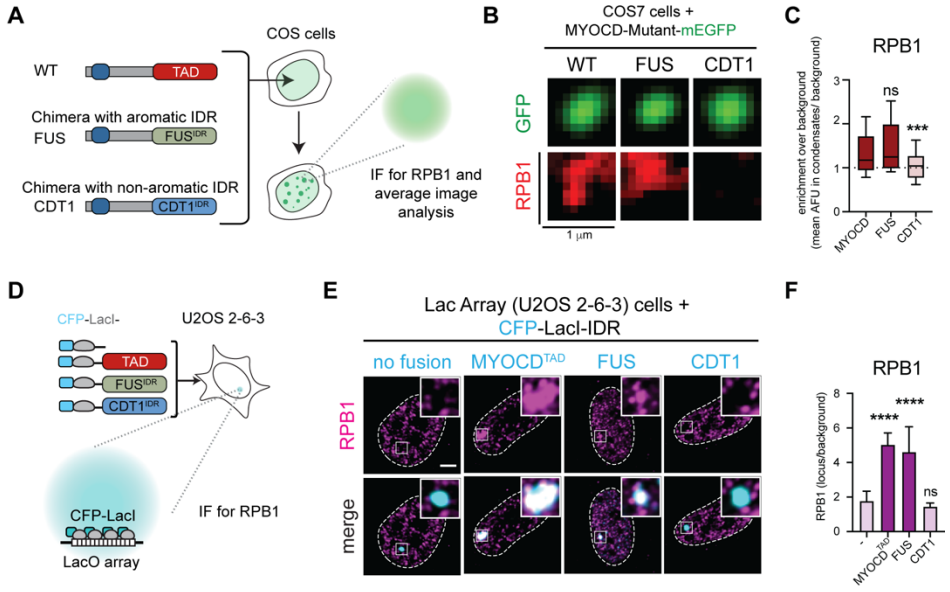

Fig. S9 Condensates formed by MYOCD TAD domain and FUS-IDR selectively partition RNA Pol II, but CDT1-IDR does not.

(A) Schematic of experimental design for colocalization of RNA Pol II (RPB1) in MYOCD condensates. **(B)** Average projection of WT MYOCD or Chimeric condensates in COS-7 cells with IF for endogenous RPB1. Scale, 5 µm. **(C)** Box plot (10%-90%) displaying the enrichment of RPB1 at the center of the MYOCD condensates normalized to background intensity. p value is from one-way ANOVA with Dunnett's multiple comparison test (p values: ns p>0.05, *** p<=0.001). n=~25. **(D)** Schematic of Lac array cells. **(E)** IF for RPB1 (magenta) in Lac array cells expressing indicated CFP-LacI fusion. Inset is LacO locus (white shows magenta and cyan overlap). Scale, 5µm. **(F)** IF Bar chart (mean ± SD) quantifying enrichment of RPB1 at CFP-LacI (no fusion) or CFP-LacI with fusion (x-axis label). p values from one-way ANOVA with Dunnett's test. (p values: ns p>0.05, **** p<=0.0001). n=22.

Fig. S10

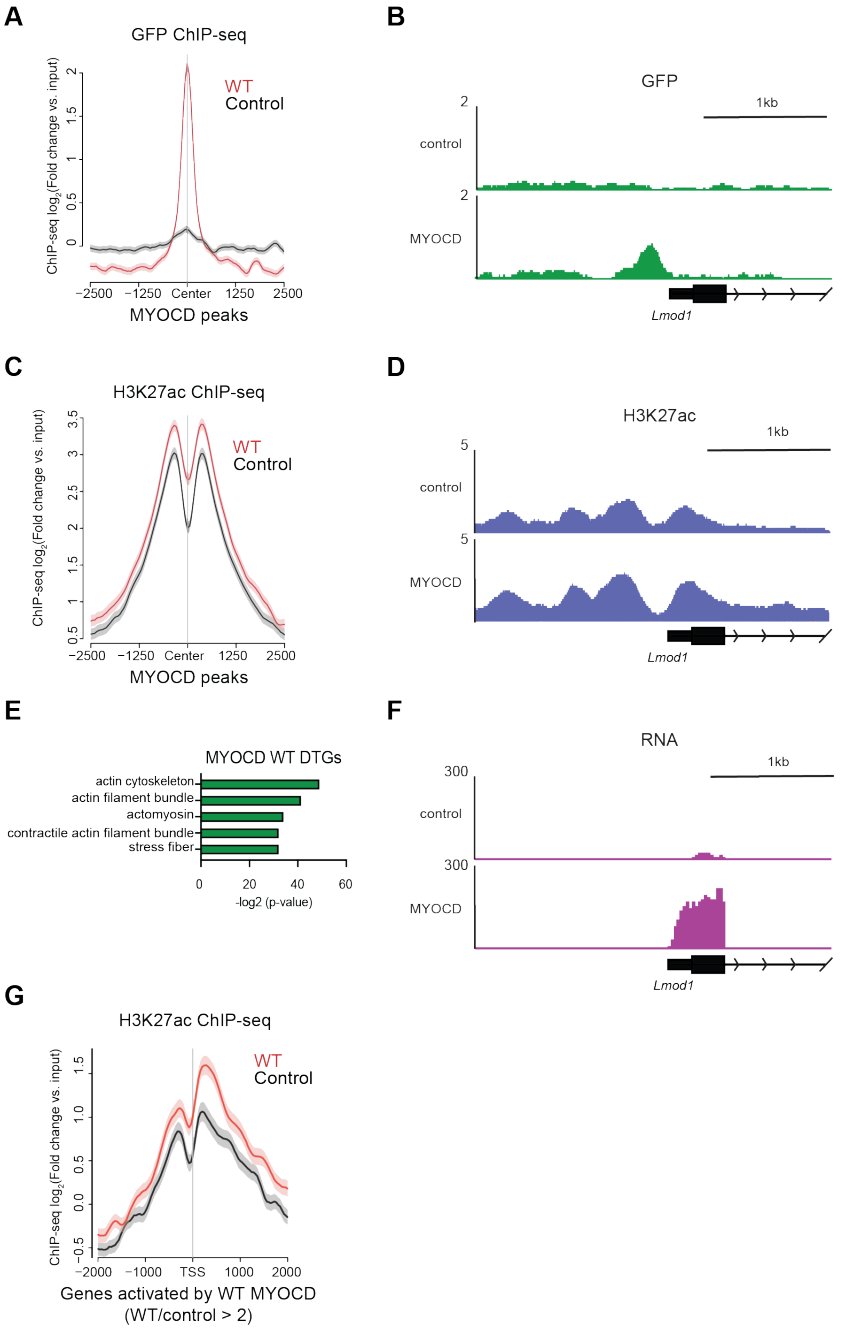

Fig. S10 MYOCD correlates with increased H3K27ac occupancy and gene expression.
(A and **C)** Metagene plot of the log_2Fold Change compared to input control of H3K27ac **(a)** or MYOCD **(c)** occupancy centered at MYOCD peaks. **(B**, **D** and **F)** Gene tracks of mEGFP and H3K27ac ChIP-seq and RNA-seq from differentiated 10T1/2 cells expressing WT MYOCD or the empty vector control. **(E)** Panther GO analysis for cellular component of WT MYOCD direct target genes. **(G)** Metagene plot of the log_2Fold Change compared to input control of H3K27ac occupancy centered at the transcription start site of genes activated by WT MYOCD.